Proceedings World Geothermal Congress 2015
Melbourne, Australia, 19-25 April 2015

New Concept for the Application of Outcrop Analogue Data for Geothermal Probability of Success (POS) Studies - Examples of Projects in the Northern Upper Rhine Graben (Germany)

Kristian Bär and Ingo Sass

Technische Universität Darmstadt, Geothermal Science and Technology, Schnittspahnstrasse 9, 64287 Darmstadt

baer@geo.tu-darmstadt.de

Keywords: Resource assessment, POS study, deep geothermal systems, outcrop analogue study, Upper Rhine Graben

ABSTRACT

Probability of success (POS) studies for deep geothermal projects are based usually on hydraulic test data of wells located in the same reservoir system in a comparable regional setting. Based on this fact prospective risk insurances ('Fündigkeits'insurance), which are often an important economic prerequisite for geothermal power projects in Germany, are not available for geothermal greenfield projects, where almost no drilling or hydraulic information of the reservoir are available.

To bypass this problem, which is partly responsible for the slow progress of the development of geothermal power production in Germany, we propose an alternative form of POS studies based on suitable outcrop analogue data. Based on a vast data base of thermophysical rock properties (more than 9,000 measurements) and hydraulic test data sets (more than 1,500 tests) sampled east and west on the Graben shoulders, borehole temperature measurements (more than 2,500 measurements) and a 3D geological model, a detailed geothermal model of the northern Upper Rhine Graben was established. This regional model, which incorporates important fault systems within the Graben and their influence on the depth and temperature dependent geothermal and hydraulic properties of different reservoir formations, is used for a local calculation of the POS. We demonstrate the usability of this probabilistic model to determine the POS for different actual project locations within the northern Upper Rhine Graben and discuss statistic uncertainties and inferred explorations risks for different locations.

1. INTRODUCTION

Investors usually require POS studies to decide whether an investment for a deep geothermal project is economically viable or not. The same applies for insurance companies that need POS studies to decide whether prospective risk insurance for the success of a geothermal well ('Fündigkeitsversicherung') with attractive conditions for the project developer is possible. Therefore, a POS study is a key for the realization of a deep geothermal project if the equity of the project developer is insufficient. This problem is partly responsible for the slow progress of the development of deep geothermal projects for electricity generation or the utilization of direct heat in the low enthalpy regions of Europe. In Germany, so far POS studies for geothermal projects are generally based on the results of deep wells in the same reservoir in the immediate vicinity of the project to be developed. For regions and reservoirs where no wells have been drilled into the reservoir formation - so called green fields - this classic approach for POS studies is not possible. Based on the example of the federal state of Hesse in Germany a new alternative approach for POS studies is proposed, which fully relies on the combination of geothermal rock parameters derived from suitable outcrop analogue studies, geological 3D modelling and temperature modelling.

Comprehensive data sets about the potential deep geothermal systems of Hesse so far only existed for the underground temperature in the region of the Upper Rhine Graben which is only a small part of the state area (Fig. 1). In addition to temperature, the bulk permeability of the reservoir, the achievable flow rate of thermal water, is the main factor of influence on the deep geothermal potential for open systems. Additionally, matrix permeability, porosity and thermal conductivity are important factors to estimate the conductive and convective heat flows within the reservoir. For assessment of the deep geothermal potential, knowledge of geological structure and geothermal properties of potential reservoir rocks are indispensable. None of the above mentioned parameters were available for the identified reservoir formations and therefore had to be collected state-wide in bibliographic, archive and most importantly in outcrop analogue and drill core investigations. This was performed in the context of the project "3D-modelling of the deep geothermal potentials of Hesse" (Sass and Hoppe, 2011; Arndt, 2012 and Bär, 2012) which was initiated in 2008 with the aim to identify and evaluate systematically the deep geothermal potential of Hesse. The established vast database could then be connected with the 3D structural model and the underground temperature model for parameterization with thermophysical and hydraulic properties.

The resulting geological-geothermal 3D model allows for a comprehensive evaluation of all deep geothermal potential reservoirs of Hesse and is capable to display the potential for open systems like hydrothermal or petrothermal (EGS) systems as well as for closed systems like deep borehole heat exchangers (Bär et al., 2011). Additionally, it provides detailed characteristics of the geothermal reservoir needed for probabilistic modelling which is the basis for POS studies without the need of direct information from deep wells in the reservoir of interest.

2. GEOLOGICAL 3D MODEL

3D modelling was conducted using the GOCAD software and techniques (Mallet, 2002). The model area covers more than 21,000 km² and has a depth of 6 km (Figure 1). The model consists of the stratigraphic units Quaternary/Tertiary in a combined unit, the mesozoic Muschelkalk (mainly limestones and marls) and Buntsandstein (sandstones, conglomerates and pelites), the paleozoic Zechstein (limestones, dolomites and evaporites), Permocarboniferous (sandstones, conglomerates, pelites and volcanics) and the Pre-Permian basement. The crystalline and metamorphic basement was divided according to the internal zones of the

Variscan Orogen (Kossmat, 1927) into the Mid-German Crystalline Rise (MGCR) in the southeastern part of Hesse, which mainly consists of felsic granitoids and subsidiary of metamorphic and basic intrusive rocks and the Rheno-Hercynian, and Northern Phyllite Zone (RH & NPZ) in the northwest, consisting of low-grade metamorphic phyllites, shists, quartzites and greywackes originating from pelagic to hemipelagic as well as volcanoclastic rocks (Figure 1 andFigure 2).

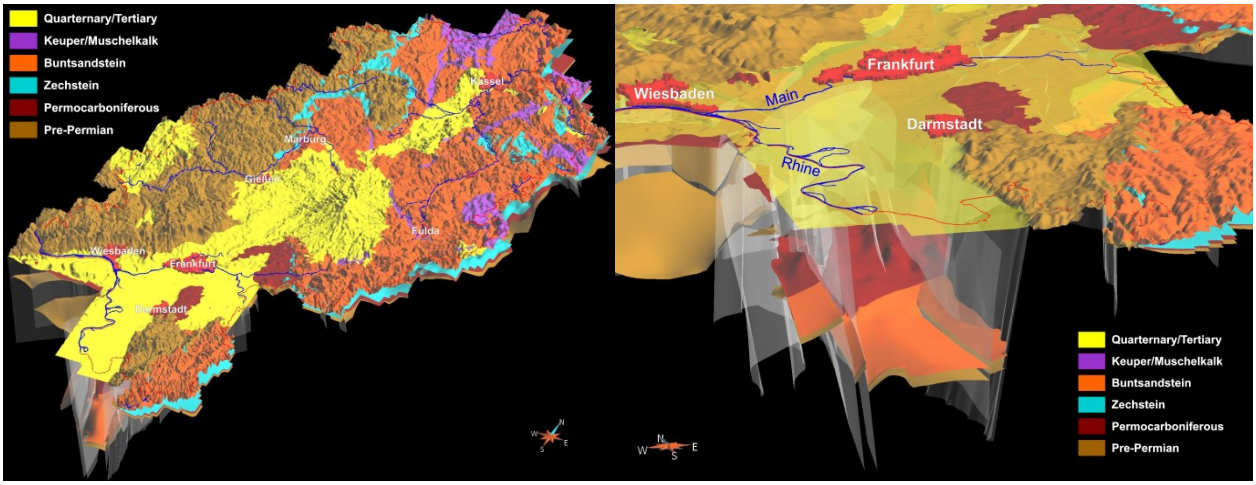

Figure 1: Overview of the geological 3D model of Hesse showing the extent and the model units as well as major fault systems (transparent grey) (left). Detail of the geological 3D model showing the area of the northern Upper Rhine Graben with the potential hydrothermal reservoir units Buntsandstein and Permocarboniferous bounded by the graben faults (right). The location of major cities (red) and rivers (blue) are given for orientation

The geological model of Hesse (Arndt, 2012) is based on the geological survey map 1:300,000 (GÜK 300; HLUG, 2007). Additional input data, e.g. well data, geological cross-sections, isopach, contour and paleogeographic maps as well as existing structural 3D models, were used (Figure 2).

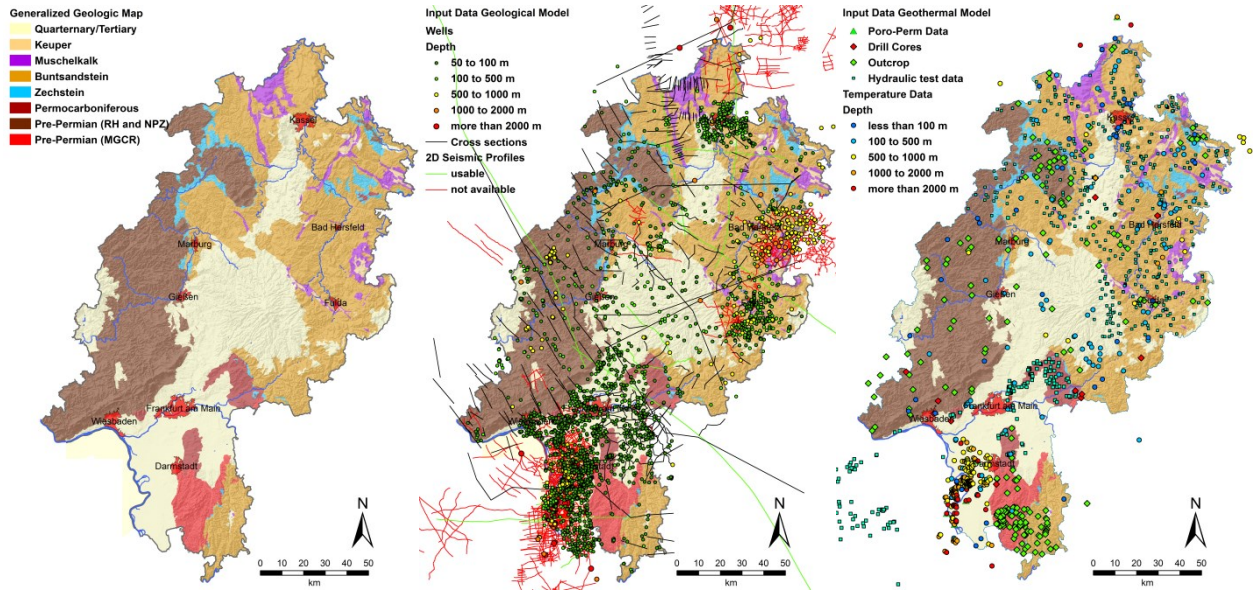

Figure 2: Generalized geological map of Hesse (left). Input data for the geological 3D model including depth of the well data. Isopach or contour maps as well as existing 3D models which were incorporated into the model are not shown (middle). Input data used for the geothermal 3D model showing the locations of all outcrop analogue study conducted and all drill cores, temperature data points, porosity and permeability data sets and hydraulic test data sets available (right).

More than 4,150 data sets from the wellbore database of the state geological surveys of Hesse (HLUG) and Lower Saxony (LBEG) were used. Furthermore, 318 geological cross sections from geological maps and other literature with a total length of more than 3,700 km have been incorporated (Arndt et al., 2011). Besides that, more than 1,500 2D seismic profiles from hydrocarbon or potassium salt exploration campaigns were assessed of which 29 interpreted ones, published earlier within other research projects, were chosen for modelling. All faults with a vertical displacement of at least 200 m were modelled. Unlike other geological 3D models at this scale, these fault zones were not modelled as vertical planes, but with their true dip angle as observed in the field, seismic profiles or geological cross sections.

3. TEMPERATURE MODEL

For the assessment of deep geothermal potential and to decide whether a geothermal reservoir is prospective, the reservoir temperature is a key parameter. Therefore, the temperature distribution in the subsurface had to be modelled to a depth of 6 km below surface.

As the temperature data distribution is very poor for the entire federal state of Hesse (Figure 2), the subsurface temperature could not have been modelled with a pure interpolation approach (cf. Agemar, 2009). A numerical approach as described by Cloetingh et al. (2010) and Förster and Förster (2000) was not feasible at the time of modelling due to the lack of sufficient data of radiogenic heat production rates. Numerical modelling of the conduction-based temperature distribution and a comparison with the interpolated temperature distribution was performed with the data presented here subsequently by Rühaak et al. (2012).

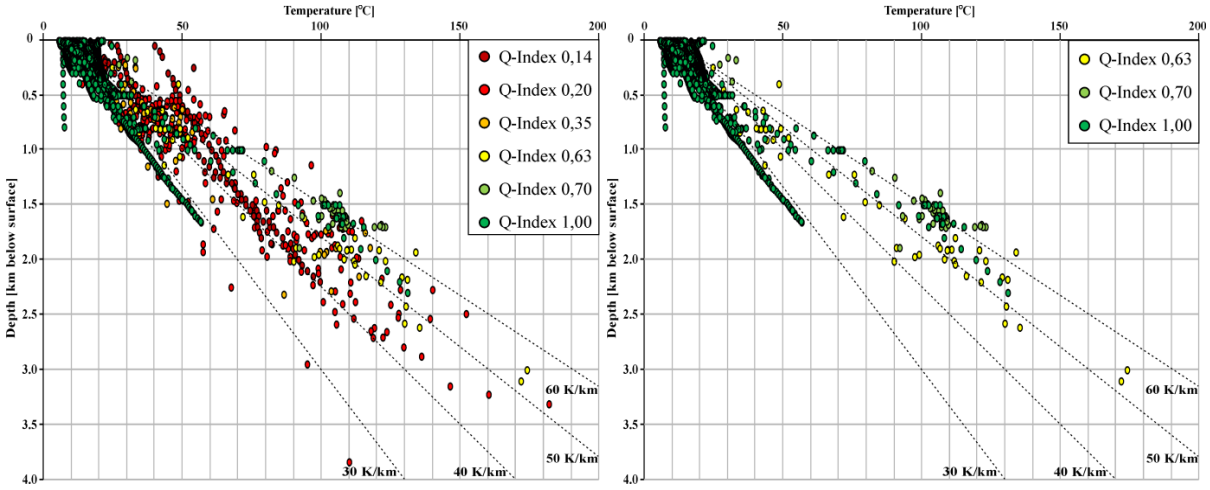

Figure 3: Temperature vs. depth plot of all available temperature data (left) and high quality data (right) for Hesse. Quality (Q)-Index as described in Table 1.

To create the first subsurface temperature model for the entire state an approach which combines interpolation supported by geologic a priori knowledge with regional geothermal gradients was chosen. Thus actual data measured in deep wells (Figure 3) was combined with the annual mean surface temperatures and regionally varying geothermal gradients derived from borehole temperature measurements in connection with the Mohorovičić Discontinuity depth map from Dèzes and Ziegler (2001) to support subsurface temperature modelling as described by Arndt et al. (2011). In ongoing studies this approach will additionally be combined with a pure conductive numerical model (Rühaak et al., 2014) which later on shall also include convective processes at major faults.

Input data were 2,029 points provided by the Geophysics Information System (FIS GP) of the Leibniz Institute for Applied Geophysics (LIAG) and the geophysics archive of the HLUG. Their depths range from 150 to 3,105 m below ground surface. Data with depths of less than 150 m have not been used due to their low relevance for deep geothermal applications and to avoid artifacts related to shallow measurements near thermal springs, seasonal influences or palaeoclimatic signals. The interpolation variogram analysis was conducted using high quality data from undisturbed temperature logs (Table 1), which were trend adjusted with a geothermal gradient of 3 K/100 m and an annual mean surface temperature of 10 °C.

Table 1: Different quality indices of temperature measurements (modified after Rühaak et al. 2012)

Quality Index	Type of Measurement	Error [K]	No.
1.00	Undisturbed Temperature Logs	0.01	1,360
0.70	Bottom Hole Temperature (BHT) with at least 3 temperature measurements taken at different times at the same depth; corrected with a cylinder-source approach	0.5	58
	Drill Stem Tests (DST)		
0.63	BHT with at least 3 temperature measurements at the same depth; corr. with the Horner-Plot Method	0.7	85
	BHT with at least 2 temperature measurements taken at different times at the same depth; corr. with an explosion line-source approach		
0.35	BHT with one temperature measurement, known radius and time since circulation (TSC)	1.6	46
	BHT with one temperature measurement, known TSC		
0.20	Disturbed Temperature Logs	2.4	200
0.14	BHT with one temperature measurement, known radius	3.0	280
	BHT with one temperature measurement, unknown radius and unknown TSC		

The resulting subsurface temperature model fits the temperature measurements, which reach a maximum depth of 3,105 m inside and 1,658 m outside the Upper Rhine Graben within a range of about ±10 K. Inaccuracies might still occur in areas where temperature data are sparse, missing or where temperature data were measured in hydrothermal convection zones. However, this model allows an improved prognosis of the temperature in the subsurface with an overall dependent depth accuracy of ± 5 K/km and can be used to create temperature maps for various depths as well as maps of depth of various isotherms (Figure 4).

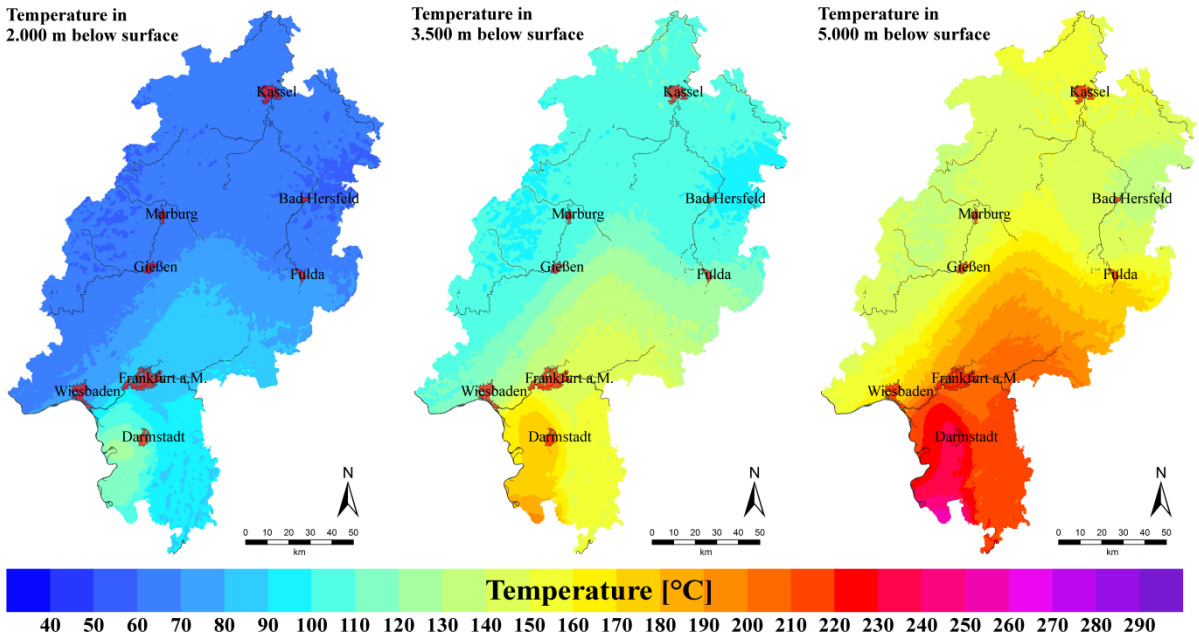

Figure 4: Maps of the modelled subsurface temperature in 2,000 m, 3,500 m and 5,000 m below surface respectively as an sample output of the temperature model. Anomalously high subsurface temperatures occur in the northern Upper Rhine Graben in the southwestern part of Hesse

4. GEOTHERMAL MODEL

Permeability and thermal conductivity are key parameters in geothermal reservoir characterization (Tester et al., 2006). The number of previous publications and databases where more than one key parameter was measured on the same sample is very low. According to the thermo-facies concept by Sass and Götz (2012) all geothermal parameters were determined in one coherent approach on the same set of samples for each facies type.

4.1 Input data

To allow predictions of the geothermal properties, a data set of outcrop analogue studies of more than 600 locations, borehole data of more than 25 boreholes and core investigations of more than 500 m of cores as well as hydraulic test data of more than 900 boreholes has been compiled for all relevant formations (Figure 2 (right)).

Systematic measurements of thermophysical and hydraulic rock properties such as thermal conductivity, thermal diffusivity, heat capacity, density, porosity and permeability were conducted on oven dry samples for each sample respectively (Bär et al., 2011). Thus a vast geothermal database of more than 25,000 measurements altogether has been created. Due to the large number of measurements the database is ideal for statistical analysis of each parameter (Table 2), to evaluate the type of statistical distribution functions of each parameter, and for correlation analysis between different parameters. The results of the statistical analysis allow calculations of the probability of occurrence and suit well the exploration risk analyses. Furthermore, the results of the statistical analyses are ideal for probabilistic modelling.

Thermal conductivity and thermal diffusivity were measured using an optical thermo scanning device. Density and porosity were investigated using a helium pycnometer and a powder pycnometer to measure both the grain density and bulk density of each sample and thus be able to calculate porosity. Matrix permeability was measured with a combined probe- and column-gas-permeameter able to measure both apparent and intrinsic permeability sensu Klinkenberg (1941). Heat capacity was not measured directly, but calculated for each sample using the Debye-Equation:

$$\rho_r = \frac{\lambda}{c_r \cdot \alpha} \tag{1}$$

where ρ_r is the density [kg·m^{-3}]; c_r, specific heat capacity [J·kg^{-1}·K^{-1}]; λ, thermal conductivity [W·m^{-1}·K^{-1}] and α, thermal diffusivity [m²·s^{-1}].

The error of the optical scanning as well as density and porosity measurements does not exceed 3 %. The error of permeability measurements is dependent on the order of magnitude of the permeability (Bär et al., 2011). The total error increases from 5 %

above K = 1 · 10^{-13} m² to about 400 % at K = 1 · 10^{-18} m². Considering the purpose of this approach and alternative measurement methods in low permeable rock, an order of magnitude is deemed a satisfactory accuracy.

All measurements were conducted on oven-dried samples to achieve the required reproducibility of results. Thus, depending on the lithology, the measurement error is significantly reduced. To transfer these data to reservoir conditions many correction approaches for saturated conditions were discussed e.g. by Hartmann et al. (2005, and references therein). Within the project the theoretical approach of Lichtenecker was chosen:

$$\lambda_r = \lambda_{fluid}^{\phi} \cdot \lambda_{matrix}^{n-\phi} \quad (2)$$

where λ_r is the thermal conductivity of the reservoir [W·m^{-1}·K^{-1}], λ_{fluid} of the fluid [W·m^{-1}·K^{-1}], λ_{matrix} of the matrix [W·m^{-1}·K^{-1}] and Φ the porosity [-].

Table 2: Extract of the geothermal database for all modelled units showing the arithmetic mean, ± standard deviation and number of measurements (n) for thermal conductivity λ, thermal diffusivity α, specific heat capacity c_p, matrix permeability K_m and bulk rock permeability K_b.

Model Units/ *Lithotypes*		λ [W·m^{-1}·K^{-1}]		n	α [mm²·s^{-1}]		n	c_p [J·kg^{-1}·K^{-1}]		n	K_m [log m²]		n	K_b [log m²]		n
		mean	σ		mean	σ		mean	σ		mean	σ		mean	σ	
Tertiary Basalts		1.81	0.26	329	0.9	0.12	267	683	90	419	-16.0	1.0	364	-	-	-
Muschelkalk		2.01	0.39	316	1.19	0.27	135	675	88	125	-16.1	0.8	309	-12.9	0.6	-
Buntsandstein		2.57	0.47	2,140	1.55	0.37	773	705	90	1,029	-13.6	1.1	2,685	-11.7	1.2	121
Zechstein		2.26	1.15	970	1.20	0.62	883	796	278	763	-15.1	1.2	958	-	-	-
Permocarbon.		2.21	0.67	1,438	1.29	0.60.	866	758	160	590	-14.1	1.4	882	-12.4	0.8	394
Basement	RH & NPZ	2.71	1.12	2,105	1.96	1.64	1,190	648	150	1,512	-15.8	1.0	1,386	-16.9	2.3	-
Basement	MGCR	2.40	0.38	1,176	1.19	0.24	1,005	755	75	966	-16.4	0.9	926	-16.4	1.7	-
				8,474			**5,119**			**5,404**			**7,599**			

4.2 Model parameterization

Parameterization of a geological 3D model requires volumetric 3D objects and not only 2D surfaces of geological horizons and faults. Therefore, GOCAD object stratigraphic grid (s-grid), for which an infinite amount of cell based properties (e.g. specific heat capacity) can be defined, was chosen. Furthermore, the s-grid can be fitted to the geological horizons and can be cut by fault surfaces exactly and has no constraints on the size of its cells (Mallet, 2002). How to build s-grids is described in general by Mallet (2002) and in the special case of this project in detail by Arndt (2012).

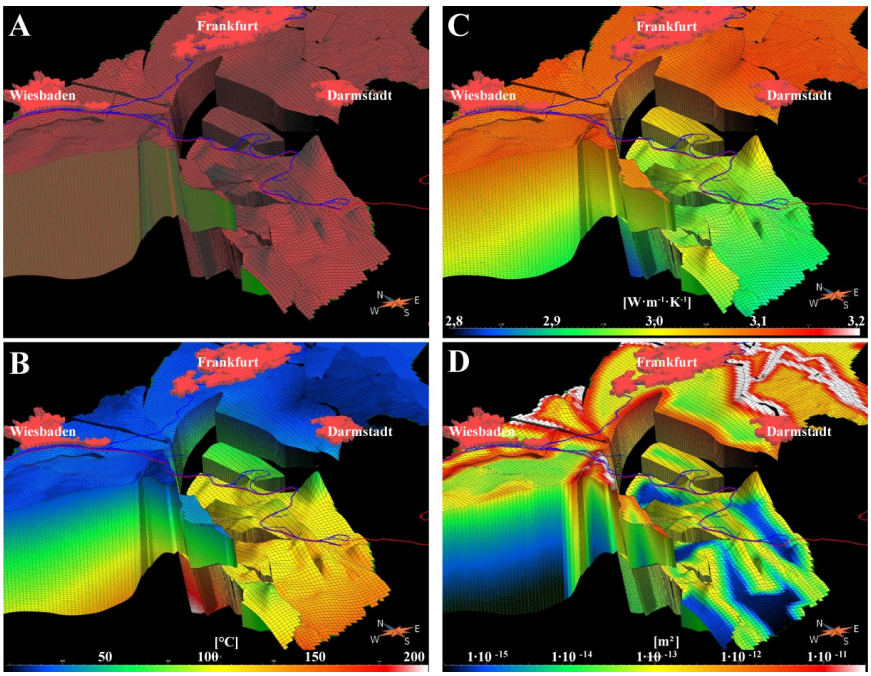

Figure 5: S-grid of the Permocarboniferous (A) parameterized depth and temperature corrected with temperature (B), thermal conductivity (C) and bulk permeability (D), including the influence of fault systems on the bulk rock permeability.

Since both hydraulic and thermophysical properties strongly depend on the in situ conditions of the reservoir, the values for saturated conditions derived from lab and field data needed to be adapted considering the temperature and pressure within the reservoir. Therefore, the outcrop analogue data was compared with in situ data from deep hydrocarbon exploration wells to develop empiric functions for the depth and temperature dependence of the hydraulic properties (Bär, 2012), which are consistent with comparable dependencies derived by other studies (Welte et al., 1997; Ingebritsen & Manning, 1999; Manning and Ingebritsen, 1999; Stober and Bucher, 2007). For the thermophysical properties established functions from crustal scale thermal models were used for adaptation to reservoir conditions (Zoth and Haenel, 1988; Somerton, 1992; Pribnow, 1994; Vosteen and Schellschmidt, 2003; Adulagatova et al., 2009).

Using these equations and the temperature model, different s-grids of the model were parameterized directly in GOCAD with properties corrected by depth and temperature: thermal conductivity, thermal diffusivity, density, specific heat capacity, porosity, matrix permeability and bulk rock permeability. Additionally, in a general approach bulk rock permeability was gradually increased in the vicinity of fault systems towards the fault by two orders of magnitude to account for the positive effect of the fault damage zones on the hydraulic properties (Caine et al., 1996; Evans et al., 1997; Faulkner et al., 2010). The in situ stress field based on the world stress map data of Heidbach et al. (2010), which is included into the 3D model, was not considered for this approach since no sufficient data of mechanical rock properties was available. Finally transmissibility was calculated based on the fault corrected bulk rock permeability and the vertical thickness of the model units.

To account for the statistic variation of all parameters in the geothermal model, for each parameter not only a mean value but also a minimum and maximum value was used for parameterization. These values are based on statistical analyses of each parameter for each geothermal model unit, which proved that all parameters either follow a normal distribution or, in case of the permeability, a log-normal distribution (Fig. 6). To exclude outliers from the parameterization, not the real minimum and maximum values were used but either the mean, ± the standard deviation, or the 1st and 3rd quartiles were used instead (for details see Bär, 2012).

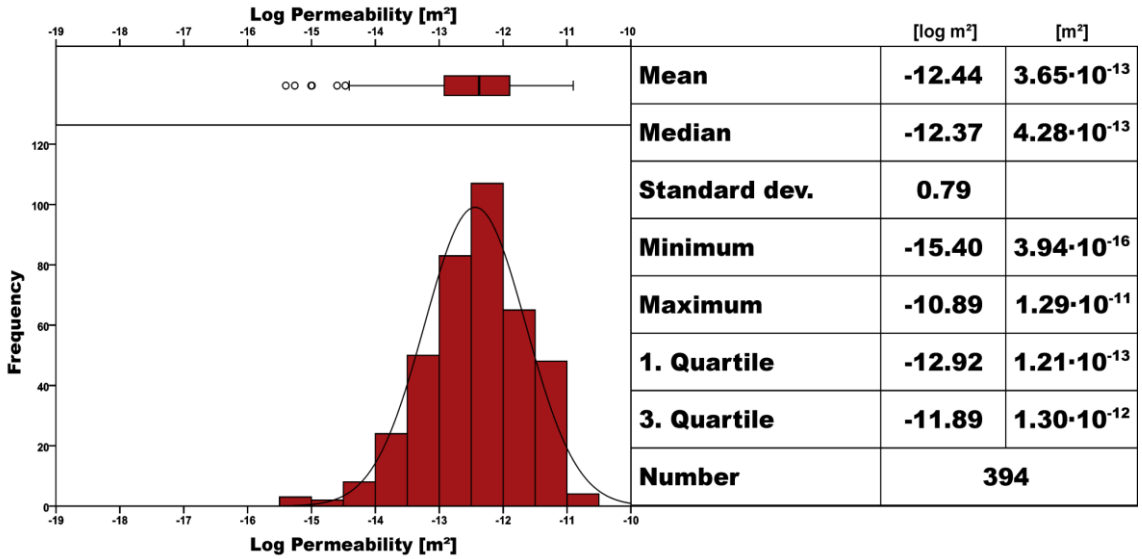

	[log m²]	[m²]
Mean	-12.44	$3.65 \cdot 10^{-13}$
Median	-12.37	$4.28 \cdot 10^{-13}$
Standard dev.	0.79	
Minimum	-15.40	$3.94 \cdot 10^{-16}$
Maximum	-10.89	$1.29 \cdot 10^{-11}$
1. Quartile	-12.92	$1.21 \cdot 10^{-13}$
3. Quartile	-11.89	$1.30 \cdot 10^{-12}$
Number	394	

Figure 6: Histogram, box-whisker-plot and statistical parameters of the bulk rock permeability of the Permocarboniferous reservoir unit which clearly follows a log-normal distribution.

4.3 Probabilistic model parameterization and geothermal potential evaluation method

In addition to the exact position of the different geological units, physical parameters have uncertainties or are inaccurate because exact information is missing in many cases. Thus physical properties of geothermal reservoir units can never be described properly by one single specific value. Based on the database described above, the distribution functions of most parameters are well known. To quantify the influence of the variation of different parameters on the results of the geothermal model, the parameter variation using Monte-Carlo Method (Deutsch, 2002; Sachs, 2003) is a helpful option. This option was included into the GOCAD based geothermal model with a GOCAD plug-in developed by Arndt (2012). The plug-in performs a large number of geothermal potential evaluations varying randomly the parameters. The variation of the parameters is based on their distribution function. If the result is a normal distribution it can be used directly for probability calculation. For the prognosis of hydrothermal and petrothermal potential the general approach was used as described by Bär et al. (2013) and Bär and Sass (2014). The approach classifies the potential in very low, low, medium, high or very high based on a weighted multi-criteria analysis of all parameters which are defined as relevant in this study.

For the plug-in, normal and log normal distributions have been implemented because all the parameters follow one of these two kinds. To describe these distributions the expected value μ and the standard deviation σ are sufficient. Normal distributions can also be described by the minimum value x_{min}, the maximum value x_{max} and the confidence level k which can be used to calculate the expected value:

$$\mu = x_{\min} + \left(\frac{x_{\max} - x_{\min}}{2}\right) \tag{3}$$

Using the error function, the cumulative probability of random normal distributions can be calculated (Sachs, 2003). This is necessary to calculate the standard deviation based on the confidence level and the expected value:

$$erf(z) = \frac{2}{\sqrt{\pi}} \int_0^z e^{-\tau^2} d\tau \tag{4}$$

$$F(x) = \frac{1}{2}\left(1 + erf\left(\frac{x-\mu}{\sigma\sqrt{2}}\right)\right) \tag{5}$$

Introducing the minimum value and the confidence level in eq. 5, we come up with eq. 6 which can be solved to eq. 7:

$$\frac{1-k}{2} = \frac{1}{2}\left(1 + erf\left(\frac{x_{\min}-\mu}{\sigma\sqrt{2}}\right)\right) \tag{6}$$

$$k = -erf\left(\frac{x_{\min}-\mu}{\sigma\sqrt{2}}\right) \tag{7}$$

To finally calculate the standard deviation, the value z is needed which delivers the result k of eq. 4. These values can be pre-calculated for certain k values for later use. For k=0.95 for example z=1.95995. Consequently, this results in:

$$z = -\frac{x_{\min}-\mu}{\sigma\sqrt{2}} \tag{8}$$

$$\sigma = -\frac{x_{\min}-\mu}{z\sqrt{2}} \tag{9}$$

These calculated values for μ and σ define a normal distribution of a parameter for a specific cell within the 3D model (Fig. 7).

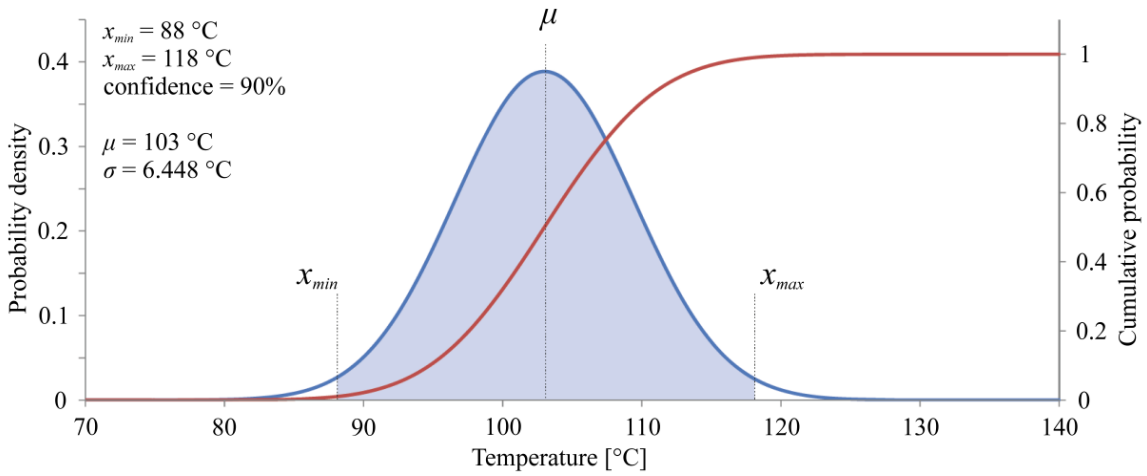

Figure 7: Distribution of subsurface temperatures of one grid cell, calculated based on the minimum x_{min} and maximum values x_{max} and the confidence level μ (modified after Arndt, 2012).

The values for the different parameters which shall be varied for the probabilistic potential evaluation are generated randomly with the Box-Muller-Method (Box and Muller, 1958). Since a log-normal distribution can easily be transformed into a normal distribution, all parameters can be simulated with the same method.

In general this evaluation can be performed for every cell of the model grid which can, based on the number of cells, parameters and scenarios simulated, result in large computational time (the grid of the reservoir unit Permocarboniferous has more than 27 million cells). To simplify the assessment a statistical analysis is implemented into the plug-in. It then calculates the arithmetic mean, the median and the standard deviation of the potential evaluation results. In addition, the percentage share of each potential class within the various scenarios can be calculated.

Based on the assumption that the result is following a normal distribution as well, additional result assessment options are possible. The hypothesis of a normal distribution can be verified by tests like the Shapiro-Wilk-Test (Royston, 1992; Shapiro and Wilk, 1965) or the Jarque-Bera-Test (Jarque and Bera, 1980). Nonetheless, these tests do not replace a detailed data analyses to verify a normal distribution. For the 3D model this is very difficult to perform because it would have to be done for every cell of the model separately.

As mentioned earlier, the following options to assess the scenarios are only viable if normal distributions are proved. The probability that a certain cell is part of a certain geothermal potential class is described by the integral of the respective normal

distribution from the lower to the upper boundary of each potential class. Since eq. 5 can be used to calculate the integral of a normal distribution $N(\mu,\sigma)$ from $-\infty$ to x (Sachs, 2003), the probability that a certain cell lies within a potential class with the lower boundary g_{min} and the upper boundary g_{max} can be calculated:

$$P(g_{\min}, g_{\max}) = \frac{1}{2}\left(1 + erf\left(\frac{g_{\max} - \mu}{\sigma\sqrt{2}}\right)\right) - \frac{1}{2}\left(1 + erf\left(\frac{g_{\min} - \mu}{\sigma\sqrt{2}}\right)\right) \quad (10)$$

Additionally, the minimum and maximum geothermal potential can be specified, as upper and lower boundaries of the area where the most likely or real geothermal potential with a probability p is located. Here, the function of the cumulative probability (eq. 5) is needed again. The parameter x, which meets eq. 12 is needed.

$$0.5 \pm \frac{p}{2} = \frac{1}{2}\left(1 + erf\left(\frac{x - \mu}{\sigma\sqrt{2}}\right)\right) \quad (11)$$

This equation can be solved for:

$$\pm p = erf\left(\frac{x - \mu}{\sigma\sqrt{2}}\right) \quad (12)$$

Analog to this procedure to calculate the standard deviations based on the confidence level, the minimum and maximum value in eq. 7 and 8, the minimum and maximum geothermal potentials can be calculated. This approach may also be applied for the probability calculation of the sole different parameters. Hence their probability to fit within predefined lower and upper boundaries is calculated.

5. RESULTS

The Monte-Carlo plug-in for probabilistic geothermal potential evaluation (Arndt, 2012) can also be used for probabilistic analyses of single parameters. This supports the decision making process whether a reservoir or a distinct location is deemed prospective.

Results are shown as example for the hydrothermal potential of the Permocarboniferous units within the northern Upper Rhine Graben (Fig. 8 and 9). For these results the minimum, mean and maximum values of the geothermal model which give information about the parameter variability were used for the approach as described in section 4.3. Therefore the confidence level was estimated to be 65 % for each parameter. Exception is the temperature where the confidence level becomes 95 %.

For potential determination into the five equidistant classes (very low, low, medium, high and very high) the threshold values (Bär et al., 2013, tab. 4) and the potential curves for each parameter (Bär, 2012) were used to demonstrate plausibility to previous results. 400 scenarios were calculated to gain a representative statistic progression of the results. In addition a Shapiro-Wilk-Test (significance level α of 5%) was performed for each model cell to validate for normal distributions.

For all cells above 2 km b.s.l. the results show a normal distribution while all cells below 2 km b.s.l. show no normal distribution, but a left or right skewness. Nonetheless the share of each hydrothermal potential class can be defined (Fig. 8). This allows a reasonable identification of the probability of each class and also illustrates the parameter variation with smooth transitions between the different potential classes. For the deeper sections of the reservoir the hydrothermal potential is classified as being high for 60 % of all scenarios. Concluding that reservoir temperatures are high enough and hydraulic properties are satisfactory to economically generate electricity using binary power plants. The other 40% are classified as medium potential class which indicates that financial funding is required to obtain economic feasibility whereas temperature and permeability are technically still more than sufficient for electricity generation.

Additionally, for the Permocarboniferous at depth of 3 km below surface the results of minimum, mean and maximum hydrothermal potential (Fig. 9) were verified by 3D seismic surveys as well as geothermal and geomechanical modelling. These exploration results were presented by independent project planners for a specific claim within the northern Upper Rhine Graben. Preferred locations (red areas in Fig. 9) for exploration boreholes are indicated and the installation of a geothermal power plant is planned if the first borehole proves to be successful. All of these areas coincide with zones where high geothermal potentials were identified with the help of the 3D geothermal potential evaluation method of the study presented here.

6. CONCLUSIONS

In contrast to the geothermal potential classes, the critical parameters are of interest for POS studies. The statistical calculation helps deciding whether minimum criteria are reached with a high enough probability or not. Since all parameters follow normal or log normal distributions, this allows the probability calculation of a minimum bulk permeability, transmissibility or reservoir temperature required for economical electricity generation in geothermal power plants or for the use of direct heat in district heating networks.

The approach using a parameterized 3D reservoir model as presented here proves that information of deep boreholes is not crucial for POS studies. In contradiction to ordinary prospective risk insurance assessments, a set of parameters statistically evaluated allows probabilistic modelling and represents a reasonable alternative for geothermal prospects where no deep borehole data is available at the current stage of development. However it has to be considered that the data is based on results from outcrop analogue studies and from more shallow boreholes. The depth and temperature dependency of each parameter has to be quantified for the model anyway. For regions and reservoirs where no wells were drilled into the reservoir formation yet - so called green fields - this new approach for POS studies permits decisions about the insurability of projects or financing from investors. The application of the method presented here may help project developers to calculate the probability of success for distinct projects.

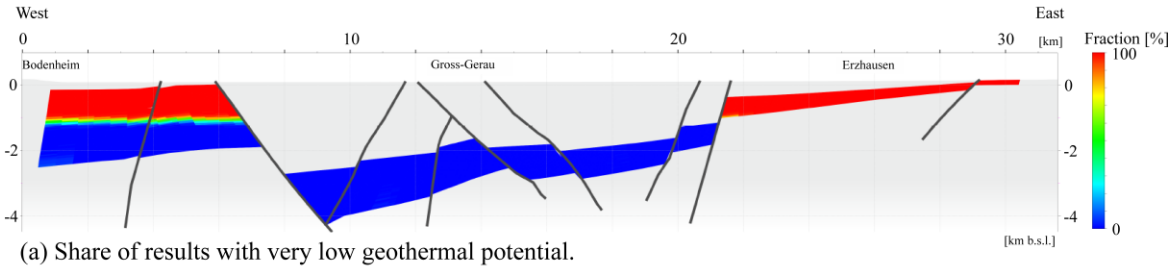

(a) Share of results with very low geothermal potential.

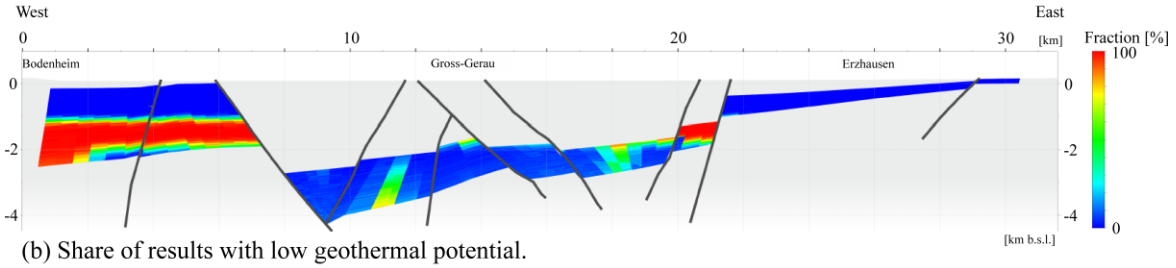

(b) Share of results with low geothermal potential.

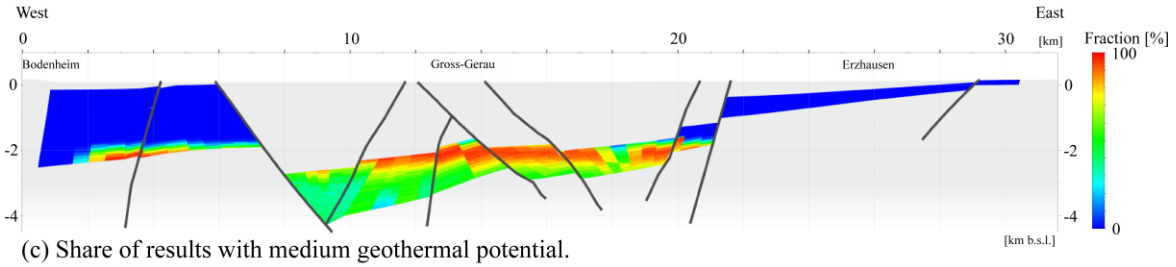

(c) Share of results with medium geothermal potential.

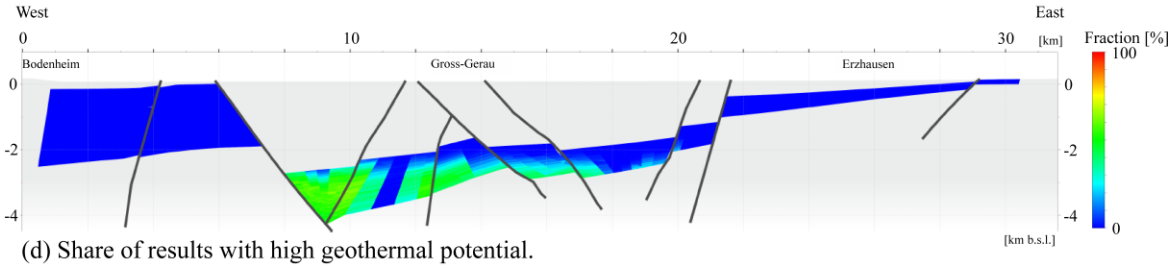

(d) Share of results with high geothermal potential.

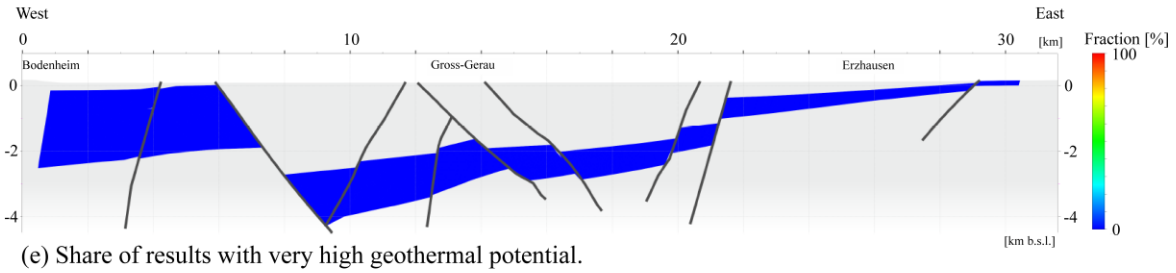

(e) Share of results with very high geothermal potential.

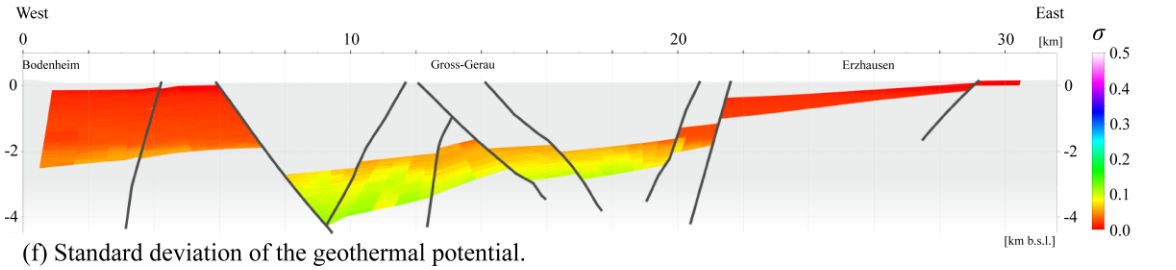

(f) Standard deviation of the geothermal potential.

Figure 8: West-East cross section of the probabilistic results of geothermal potential evaluation for the Permocarboniferous reservoir unit within the northern Upper Rhine Graben (a-e) and the corresponding standard deviation for the potential classes (each class has a range of 0.2) (f) (modified after Arndt, 2012).

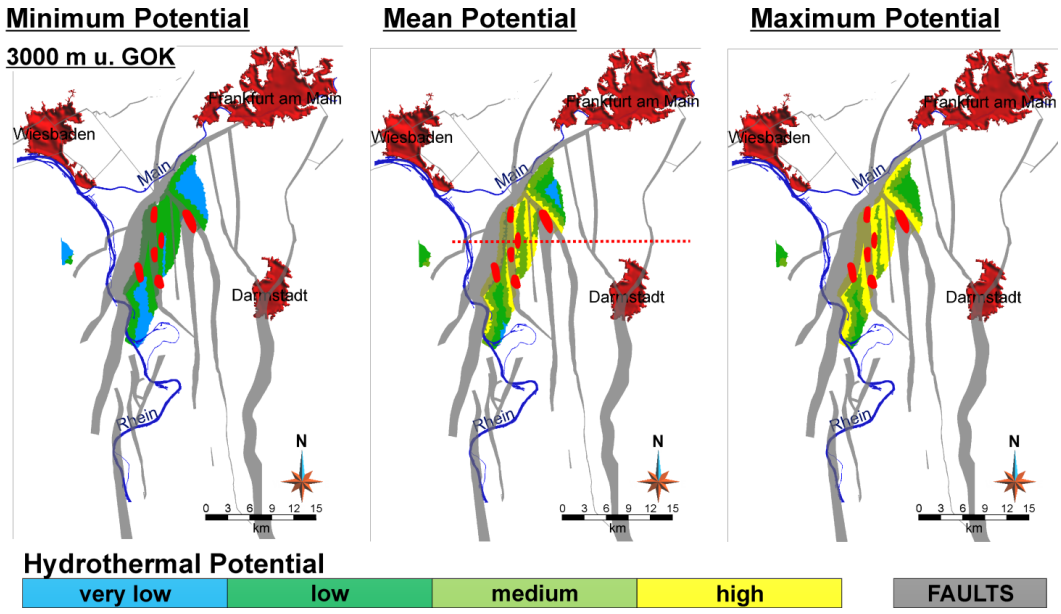

Figure 9: Map of minimum, mean and maximum hydrothermal potential of the Permocarboniferous in the northern Upper Rhine Graben at a depth of 3,000 m below surface including the position of the cross section shown in Fig. 8 (red dotted line). The red ellipsoids coinciding with areas of high hydrothermal potential represent preferred locations for exploration boreholes identified based on exploration results of an independent project planner. The location of major cities and rivers are given for orientation. Grey shaded areas are the modelled fault interfaces within the Permocarboniferous.

7. ACKNOWLEDGEMENTS

We kindly acknowledge the discussions with and the support of our cooperation partners in the Institute of Applied Geosciences, Dirk Arndt and Andreas Hoppe as well as our research partners of the Geological Survey of the Federal State of Hesse - HLUG (Hessisches Landesamt für Umwelt und Geologie) Johann-Gerhard Fritsche and Matthias Kracht as well as all other staff members who were involved in the project. We thank the Hessian Ministry of Environment, Energy, Agriculture and Consumer Protection (Hessisches Ministerium für Umwelt Energie, Landwirtschaft und Verbraucherschutz (HMUELV)) for funding the project. Data delivered by the Geological Survey of Hesse (HLUG), of Lower Saxony (LBEG) and of Rhineland-Palatinate (LGB-RLP) as well as from the oil and gas industry (Wirtschaftsverband Erdöl- und Erdgasgewinnung e.V. (WEG)) made it possible to successfully develop the 3D geological-geothermal model for the entire Federal State of Hesse.

REFERENCES

Abdulagatova, Z., Abdulagatov, I.M., and Emirov, V.N.: Effect of temperature and pressure on the thermal conductivity of sandstone, *International Journal of Rock Mechanics & Mining Sciences*, 46, (2009), 1055-1071.

Agemar, T.: Struktur- und Temperaturmodelle, *In: Schulz, R. and GEOTIS-Team (Eds.): Aufbau eines geothermischen Informationssystems für Deutschland, Endbericht*, Hannover (2009), 82–94.

Arndt, D., Bär, K., Fritsche, J.-G., Kracht, M., Sass, I. and Hoppe, A.: 3D structural model of the Federal State of Hesse (Germany) for geo-potential evaluation, *Z. dt. Ges. Geowiss.*, 162(4), Stuttgart (Schweizerbart), (2011), 353-370.

Arndt, D.: Geologische Strukturmodellierung von Hessen zur Bestimmung von Geo-Potenzialen, *PhD thesis*, TU Darmstadt (2012), 199 p.

Bär, K., Arndt, D., Fritsche, J.-G., Götz, A.E., Hoppe, A., Kracht, M. and Sass, I.: 3D-Modellierung der tiefengeothermischen Potenziale von Hessen – Eingangsdaten und Potenzialausweisung, *Z. dt. Ges. Geowiss.*, 162 (4), Stuttgart (Schweizerbart), (2011), 371-388.

Bär, K., Arndt, D, Hoppe, A. & Sass, I.: Investigation of the deep geothermal potentials of Hesse (Germany), *Proceedings*, European Geothermal Congress (2013), Pisa, Italy. ISBN: 978-2-8052-0226-1.

Bär, K. & Sass, I.: 3D-Model of the Deep Geothermal Potentials of Hesse (Germany) for Enhanced Geothermal Systems, *Proceedings*, 39th Workshop on Geothermal Reservoir Engineering, Stanford University, Stanford, CA, February 24-26, 2014, SGP-TR-202, (2014), 208-219.

Bär, K.: Untersuchung der tiefengeothermischen Potenziale von Hessen, *PhD thesis*, TU Darmstadt, (2012), 265 p.

Box, G.E.P. & Muller, M.E.: A Note on the Generation of Random Normal Deviates, *Ann. Math. Statist*, 29.2, (1958), 610-611.

Caine, J.S., Evans, J.P., and Forster, C.B.: Fault zone architecture and permeability structure, *Geology (Boulder)*, 24, (1996), 1025–1028.

Cloetingh, S., van Wees, J.D., Ziegler, P.A., Lenkey, L., Beekman, F., Tesauro, M., Förster, A., Norden, B., Kaban, M., Hardebol, N., Bonté, D., Genter, A., Guillou-Frottier, L., Ter Voorde, M., Sokoutis, D., Willingshofer, E., Cornu, T. and Worum, G.:

Lithosphere tectonics and thermo-mechanical properties: An integrated modelling approach for Enhanced Geothermal Systems exploration in Europe, *Earth-Science-Reviews*, 102(3-4), (2010), 159-206.

Deutsch, C.V.: Geostatistical reservoir modeling, New York: Oxford Univ. Press, (2002), 376 p.

Dèzes, P. and Ziegler, P. A.: European Map of the Mohorovičić discontinuity, *In: Mt. St. Odile (eds.): 2nd EUCOR-URGENT Workshop (Upper Rhine Graben Evolution and Neotectonics)*, (2001), France.

Evans, J.P., Forster, C.B. and Goddard, J.V.: Permeability of fault-related rocks and implications for hydraulic structure of fault zones, *J. Struct. Geol.*, 19, (1997), 1393–1404.

Faulkner, D.R., Jackson, C.A.L., Lunn, R.J., Schlische, R.W., Shipton, Z.K., Wibberley, C.A.J. and Withjack, M.O.: A review of recent developments concerning the structure, mechanics and fluid flow properties of fault zones, *J. Struct. Geol.*, 32, (2010), 1557-1575.

Förster, A. and Förster, H.-J.: Crustal composition and mantle heat flow: Implications from surface heat flow and radiogenic heat production in the Variscan Erzgebirge (Germany), *J. Geophys. Res.*, 105(B12)(27), (2000), 917-938.

Hartmann, A., Rath, V. and Clauser, C.: Thermal conductivity from core and well log data, *International Journal of Rock Mechanics & Mining Science*, 42, (2005), 1042-1055.

Heidbach, O., Tingay, M., Barth, A., Reinecker, J., Kurfeß, D. and Müller, B.: Global crustal stress pattern based on the World Stress Map database release 2008, *Tectonophys.*, 482, (2010), 1–4, 3–15.

HLUG: Geologische Übersichtskarte Hessen 1:300.000, *5. revised digital edition, Hessisches Landesamt für Umwelt und Geologie* (2007), Wiesbaden.

Ingebritsen S.E. and Manning C.E.: Geological implications of a permeability-depth curve for the continental crust, *Geology*, 27, (1999), 1107–1110.

Jarque, C.M. & Bera, A.K.: E-cient tests for normality, homoscedasticity and serial independence of regression residuals, *Economics Letters*, 6.3, (1980), 255-259.

Klinkenberg, L.J.: The permeability of porous media to liquids and gases, *Drilling Production Practice, API* (1941), 200-213.

Kossmat, F.: Gliederung des varistischen Gebirgsbaues, *Abh. Sächs. Geol. Landesamt*, 1, (1927), 39 p., Leipzig.

Mallet, J.-L.: Geomodeling, Oxford University Press, Oxford, New York, (2002), VIII, 599 p.

Manning, C.E. and Ingebritsen, S.E.: Permeability of the continental crust: implications of geothermal data and metamorphic systems, *Rev. Geophys.*, 37, (1999), 127–150.

Pribnow, D.: Ein Vergleich von Bestimmungsmethoden der Wärmeleitfähigkeit unter Berücksichtigung von Gesteinsgefügen und Anisotropie, *VDI Fortschrittsberichte*, 19(75), (1994), VDI-Verlag, 111 p.

Royston, P.: Approximating the Shapiro-Wilk W-test for non-normality, *Statistics and Computing*, 2.3, (1992), 117-119.

Rühaak, W., Bär, K. and Sass, I.: Estimating the subsurface temperature of Hesse/Germany based on a GOCAD 3D structural model - a comparison of numerical and geostatistical approaches, *Proceedings* EGU 2012, Wien, (2012).

Rühaak, W., Bär, K. and Sass, I.: Combining numerical modeling with geostatistical analysis for an improved reservoir exploration, *Proceedings* EGU 2014, Wien, (2014).

Sachs, L.: Angewandte Statistik. Berlin [u.a.]: Springer, (2003), 890.

Sass, I. and Götz, A.E.: Geothermal reservoir characterization: a thermofacies concept, *Terra Nova* 24(2), (2012), 142–147. Blackwell Publishing Ltd.

Sass, I. and Hoppe, A., (eds.): Forschungs- und Entwicklungsprojekt „3D-Modell der geothermischen Tiefenpotenziale von Hessen", *Abschlussbericht*, Technische Universität Darmstadt, Darmstadt. (2011), 218 p.

Shapiro, S. S. & Wilk, M. B.: An Analysis of Variance Test for Normality (Complete Samples), *Biometrika*, 52.3/4, (1965), 591-611.

Somerton, W. H.: Thermal properties and temperature-related behavior of rock-fluid systems, *Developments in Petroleum Science*, 37, (1992), VIII: 257 p.

Stober, I. and Bucher, K.: Hydraulic properties of the crystalline basement, *Hydrogeology Journal*, 15, (2007), 213–224.

Tester, J.W., Anderson, B.J., Batchelor, A.S., Blackwell, D.D., DiPippo, R., Drake, E.M., Garnish, J., Livesay, B., Moore, M.C., Nichols, K., Petty, S., Toksöz, M.N., Veatch, R.W., Baria, R., Augustine, C., Murphy, E., Negraru, P. & Richards, M.: The Future of Geothermal Energy. - Massachusetts Institute of Technology, Cambridge, MA, (2006).

Vosteen, H.D. and Schellschmidt, R.: Influence of temperature on thermal conductivity, thermal capacity and thermal diffusivity for different types of rock, *Physics and Chemistry of the Earth*, 28, (2003), 499-509.

Welte, D.H., Horsfield, B. & Baker, D.R. (eds.): Petroleum and basin evolution: Insights from petroleum geochemistry, geology and basin modeling, Springer, Berlin, (1997), 535 p.

Zoth, G. & Hänel, R.: Appendix, In: Handbook of Terrestrial Heat- Flow Density Determination, Hänel, R., Rybach L. & Stegena, I. (eds.). - Kluwer Academic Publishers, Dordrecht, (1988), 449-466.